

Bivalent system of deoxyribozymes for efficient RNA cleavage

Michael Batsa ¹, Mikhail Dubovichenko ¹ and Dmitry M. Kolpashchikov²

¹ SCAMT Institute, ITMO University, post code city, country; kmichaelbatsa@gmail.com (M.B.); dubovichenko@scamt-itmo.ru (M.D.)

² Department of Chemistry, University of Central Florida, post code city, country; dmitry.kolpashchikov@ucf.edu

Abstract: The goal of gene therapy is to treat diseases through gene editing and gene expression modification. Viral vectors, antisense oligonucleotides (ASO) and RNA interference (RNAi) are some of the gene therapies under development. DNAzyme, or deoxyribozyme (Dz), are simple in design and simple tools for RNA-cleaving gene therapy. However, Dz affinity and efficiency remain a significant challenge to be addressed. In nature, multiple ligands bind to targets at multiple sites with high affinity and avidity resulting in effective inhibition or stimulation of biological responses. Scientists have reported multivalency in biological systems as a powerful strategy for achieving high-affinity molecular recognition. Our main goal was to improve the affinity and efficiency of DNAzyme cleaving RNA by developing and optimizing 10-23 DZ base gene therapy molecules. We used 10-23 Dz to target folded mRNA and tested their knockdown efficiency in an in vitro physiological buffer. Next, we optimized 10-23 DZ by designing monovalent DZs with varied arm lengths (short arms with 1-2 nucleotides less and long arms with 1-2 nucleotides more) to find the most efficient and stable construction and tested their efficiency in a cooperative association. It was observed that cooperative DZ1-DZ2 association was more efficient in comparison with separately working Dz1 and Dz2. Further investigation with different lengths (-/+1, +2 nucleotides) of binding arms influenced the efficiency of 10-23 Dz. The result indicated that, as the length of the binding arms increases, the efficiency also increases. This research has demonstrated that multivalent association of DNAzymes have great potential to increase DNAzyme-cleaving RNA affinity and efficiency as a therapeutic agent.

Citation: Lastname, F.; Lastname, F.; Lastname, F. Title. *Biol. Life Sci. Forum* **2022**, *2*, x. <https://doi.org/10.3390/xxxxx>

Academic Editor:

Published: date

Publisher's Note: MDPI stays neutral with regard to jurisdictional claims in published maps and institutional affiliations.



Copyright: © 2022 by the authors. Submitted for possible open access publication under the terms and conditions of the Creative Commons Attribution (CC BY) license (<https://creativecommons.org/licenses/by/4.0/>).

Keywords:

1. Introduction

To date, there are many diseases that have a genetic origin: viral and bacterial infections, genetic disorders, and cancer. Most of them are being studied by scientists, and recently, some ways to treat such diseases already exist. Examples, antibiotics against bacterial infections, interferon proteins to treat viruses or small molecules, and chemotherapy for cancer treatment [1]. To minimize off-target effects in the treatment of such diseases, more precise methods have been developed, such as gene therapy. Gene therapy aims to treat diseases through genome editing and gene expression modification [2]–[4]. Viral vectors, antisense oligonucleotides, RNA interference (RNAi), plasmids, DNAzymes (Dzs), and CRISPR/Cas9 are some of the gene therapies under development [5]. Such approaches have off-target effects, low affinity for target gene-encoding DNA/RNA [6]. Modern methods of addressing such issues include chemical modification of molecular tools and computer design. But such approaches are still being studied and do not

guarantee high therapeutic effects [7]. In this work, to increase affinity to target gene-encoding RNA, we cooperatively associate 10-23 to cleave a single target at multiple sites.

DNAzyme or deoxyribozyme (Dz) is a term used to describe single-stranded DNA molecular catalysts obtained through in-vitro screening technology [8] and can catalyze a variety of reactions, including RNA and DNA cleavage and ligation, as well as DNA phosphorylation [9]. RNA-cleaving Dzs 10-23 are known to be the most studied Dzs in gene therapy. They are made up of two parts: the substrate-binding arms and the catalytic site. The binding arms cause Dz to hybridize with the substrate, and the catalytic site catalyzes substrate cleavage with the help of metal ion cofactors such as Mg^{2+} , Pb^{2+} , Zn^{2+} , Mn^{2+} , and others.

Dzs [8], like ASO and siRNA but protein independent, act as knockdown agents at the mRNA level, suppressing gene expression [10]. Dzs have a simple design that is very promising for gene therapy. Despite their low toxicity and widespread availability, the cleavage efficiency of Dzs remains a significant challenge that must be overcome. Because of mRNA folding in the secondary and tertiary structures, the absence of a cleavage site contributes significantly to inefficient cleavage activity [11]. This research aimed to improve Dz cleavage and catalytic activity by combining different Dzs in a bivalent system.

As in nature, the concept of multivalent drugs consists of multiple ligands that bind to their target to moderate affinity at multiple sites, which results in high avidity and effective inhibition or stimulation of biological responses [12]. As original Dzs, BDs allow inhibition of expression of critical targeted genes via catalytic cleavage of mRNA, but their effectiveness is determined by avidity (which can be considered as the sum of the affinity of each active ligand containing the drug) instead of affinity, and we suppose that this parameter will increase drug-target interaction. Our objective was to optimize and cooperatively associate 10-23 Dz to cleave a single target at multiple sites and compare their catalytic activities with separately working 10-23 Dz1 and Dz2.

Many biomolecular components use multivalent interactions to overcome weak monovalent, non-covalent interactions and to strengthen their biomolecular interactions, allowing the occurrence of desired biological processes [13]. Antibodies use two antigen recognition parts for immune response; viruses utilize multivalent interactions to attach themselves to host cells (Figure 1). Natural multivalent glycoconjugates can be applied to inhibit the adhesion of viruses, bacterial toxins, and bacteria to host cells or to stimulate the innate and adaptive immune systems [14]. Ligands have poor binding properties on their own but, when linked by a scaffold, can produce a high collective affinity for a corresponding receptor with multiple binding sites. Synthetic multivalent ligands can be made to behave in several ways that mimic natural multivalent displays. They increase the chances of ligands rebinding to their binding site and lower the off-rate due to the high concentration of local ligands around the receptor. Multivalent Dzs [15] are currently receiving attention to developing efficient cleavage agents for gene therapy [16]. Multivalent Dzs have catalytic cores that facilitate the cleavage of targeted nucleic acids at specific sites. They can be conjugated end-to-end to produce more than one oligonucleotide in a single nanostructure. This approach could increase Dz hybridization to its target, thereby increasing Dz affinity. Multiple Dz in cooperative association presents multiple cleavage activity at different sites which could efficiently knockdown gene of interest.

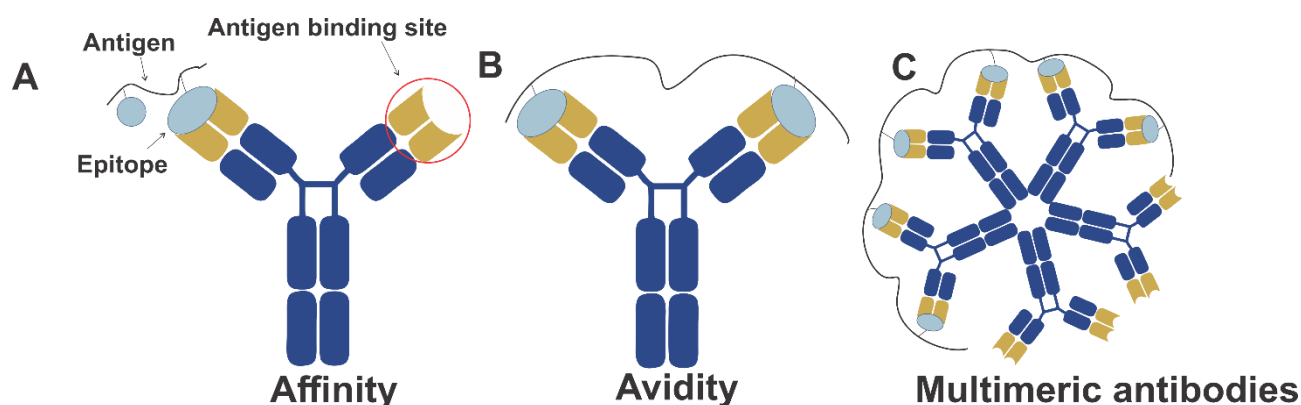


Figure 1. Antibody interaction. (A) Affinity is single ligand interaction. Antigen interaction at single antigen binding site (dark yellow variable domain) demonstrating a monovalent interaction (B) Avidity is the sum of the ligands binding interaction. Antigen interacting at 2 antigen binding sites of an antibody demonstrating a bivalent interaction. (C) Multimeric antibodies (such as IgM) increase the avidity of antibodies. CorelDRAW 2021 was used to design the image. CorelDRAW 2021 was used to design the image.

2. Materials and Method

2.1. DNA and RNA Fragments Used

Different DNA and RNA fragments were used in conducting the study (Table 1). DNA fragments constituted Dzs. Computational tool was used to design the oligonucleotides. The secondary structure, melting temperature and Gibbs energy of the mRNA (STR-58) were estimated using the mFold web server. The secondary structure of targeted mRNA is demonstrated in Figure 2. Mutation (mismatch (mm) was introduced in T1 of BD4.

Table 1. Oligonucleotides used in the experiment.

Name	Arms	Sequence	Melting Point (°C)
Dz1	X1	CATATCGGTGC	32.4
	Y1	CATGGCAAACA	34.5
Dz2	X2	CGGTAGCTCTC	34.1
	Y2	TCGAGCCGC	34.9
Catalytic core		A GGC TAG CTA CAA	

2.2. Buffers and Reagents Used

The following buffers were used in the experiment:

(1) Reaction buffer. It consisted of sodium chloride (NaCl), potassium chloride (KCl), magnesium chloride (MgCl₂), and 4-(2-hydroxyethyl)-1-piperazine ethane sulfonic acid (HEPES).

(2) TBE was made up of tris(hydroxymethyl) aminomethane (Tris base), boric acid, Ethylenediaminetetraacetic acid (EDTA).

(3) Polyacrylamide gel electrophoresis (PAGE) was prepared using acrylamide/bis-acrylamide (40% AA:BA), ammonium persulfate (APS), tetramethylenediamine (TEMED), tris borate EDTA (TBE x10) buffer, and urea.

(4) Stop buffer consisted of Urea, TBE, Bromophenol blue(optional), TEMED

Table 2. Buffers, reagents, and gels used in the experiment.

Reagents	Usage	Company
Oligonucleotides	For building DNA constructs	DNAsynthesis
Fluorescent Substrate	Produce a fluorescent signal after detection of the nucleic acids	DNAsynthesis
Oligonucleotides	For building DNA constructs	DNAsynthesis
Fluorescent Substrate	Produce a fluorescent signal after detection of the nucleic acids	DNAsynthesis
H2O RNAse Free	Dilution of Oligo's and buffer preparation	QIAGEN
KCl,	Cleavage buffer preparation	ROTH
MgCl ₂ ,	Cleavage buffer preparation	ROTH
HEPES	Cleavage buffer preparation	ROTH
NaCl	Cleavage buffer preparation	ROTH
Hepes	Cleavage buffer preparation	ROTH
Tris	TBE buffer preparation	Helicon
Boric acid	TBE buffer preparation	Helicon
EDTA	TBE buffer preparation	Helicon
Acrylamide (AA)	PAGE preparation	Helicon
Bis-acrylamide (BA)	PAGE preparation	Helicon
APS	PAGE preparation	
Urea	Stop buffer and PAGE buffer preparation	ROTH
TEMED	Stop buffer and PAGE buffer preparation	
Bromophenol blue (optional)	Stop buffer preparation	
Ethidium Bromide	Staining nucleic acid	
Molecular rulers	DNA ladders	Everogene
Loading buffer 4x, 6x	Sample loading	Everogene

2.3. Experimental Procedure

2.3.1. Cleaving RNA and Cleavage Agents

1 μ M of RNA STR-58 (Figure 2) was incubated with different concentration (10, 25, 50, 100 nM) of cleavage agents (Dzs) in a nearly physiological buffer (KCl = 150 mM, NaCl = 15 mM, MgCl₂ = 2 mM, HEPES = 50 mM, pH = 7.5) condition at 37°C at different time points (0, 0.5, 1, 2, 3, 5, 7, 10, 24 h) depending on the experiment. The reaction was stopped by adding stop buffer to the samples in the ratio 1:1 at the end of each time point.

2.3.2. PAGE Assay and Data Analysis

20% PAGE assay (40% AA:BA, TBE x10, Urea, 10% APS, TEMED) was used to detect the cleavage intensity after the experimental reaction. Samples were annealed at 95°C for 5min on a thermostat and then loaded into the wells of the gels. PAGE ran at 80 V for 3 h and 30 min and visualized in ChemiDoc. The mRNA substrates were labelled with amidite (FAM) that emit fluorescence to enable visualization. The reaction produced 2 or 3 bands depending on the cleavage agent used. The first band (initial band) is the band of the whole RNA used. Band 2 (cleavage product 1), the middle band was the largest cleavage product and band 3 (cleavage product 2), the bottom band was the smallest cleavage product. The size of the product was based on the sequence of the cleaved RNA product. Densitometry was performed by estimating the differences in fluorescence rates of the bands using a grey value measuring instrument in Adobe Photoshop. Graphs were plotted using the average value of at least three independent cleavage measurements.

Cleavage percentages were calculated in Microsoft Excel by formula (1). OriginLab was used to plot graphs using the mean and standard deviation values obtained from Excel.

$$\text{Cleavage percentage (\%)} = \frac{B+C}{A+B+C} \times 100\% \quad (1)$$

where A represents the initial RNA band intensity, B represents the largest cleavage product, and C represents the smallest cleavage product.

3. Results and Discussion

3.1. Choosing Target RNA STR-58

RNA molecules are important for cellular communication and gene regulation. Targeting these RNAs with small molecules offers opportunities to therapeutically modulate cellular processes. Knockdown of a specific target mRNA would cause gene's expression to be downregulated, resulting in therapeutic effects or antibiotic efficacy. Streptomycin MICs in *E. coli* can be considerably altered by genes encoding streptomycin resistance, and *strA-strB* genes are likely implicated in conferring high-level streptomycin resistance [17]. These genes have been found in bacteria invading plants, animals, humans, and fish, and they are widely distributed among gram-negative bacteria [18]. We employed a fragment of mRNA from the *strA* streptomycin resistance cassette with a sequence length of 58 (STR-58) for in vitro investigations (Figure 2). It has rich guanine-uracil (GU) sites that Dz can cleave, and its folding Gibbs energy is -23.4 kcal/mol, indicating it is highly stable under physiological conditions.

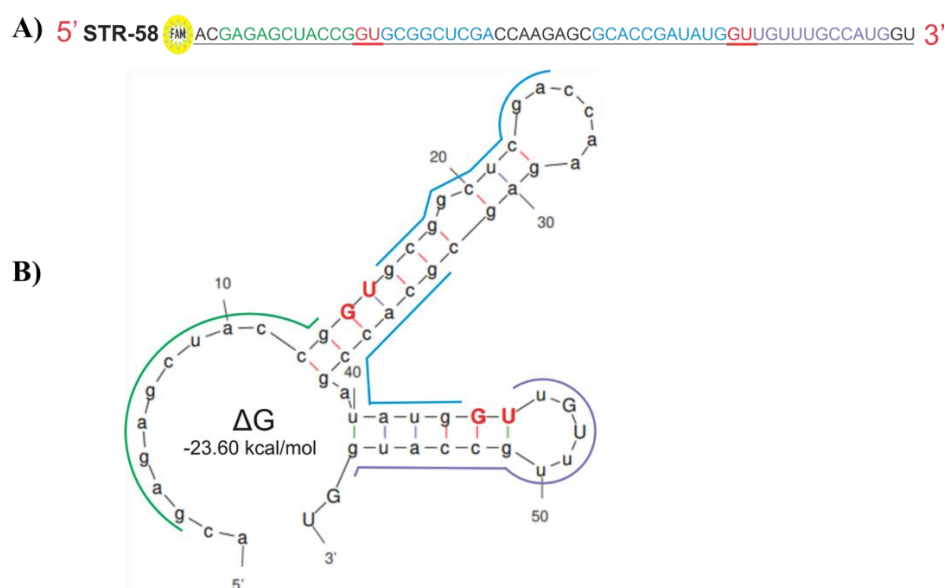


Figure 2. The structure of STR-58 fragments. (A) The sequence of RNA STR-58 with FAM-label on the 5'-end. STR-58 fragment was used as the substrate. Red letters indicate cleavage site for cleavage agents (GU). Green, blue, and purple lines are the binding sites for cleavage agent hybridization. (B) Stable secondary structure of STR-58 that mimics biological RNA. ΔG is -23.6 kcal/mol. The secondary structure was achieved by using the mFold web server (The RNA Institute-University at Albany). The website of mFold Web Server is <http://unafold.rna.albany.edu/>.

3.2. Design of Catalytic DNAzymes Used in the Study

We used regular 10-23 Dz and a modification of 10-23 Dz in accomplishing the study. Dz1 and Dz2 were two variants of Dz 10-23 that were used. The monovalent systems were 10-23 Dz strands (either Dz1 or Dz2) (Figure 3), whereas Dz1-Dz2 formed an association (multivalent) (Figure 3C). Chemical modifications were made to both Dz_{11/11} and

Dz2_9/11 by removing one nucleotide from the binding arms or adding one or two nucleotides to the binding arms (Figure 5). Dz1-Dz2 (Figure 3C) has four binding arms and two catalytic cores. Because of their association, Dz1-Dz2 cleaves at two target sites due to the presence of two catalytic cores.

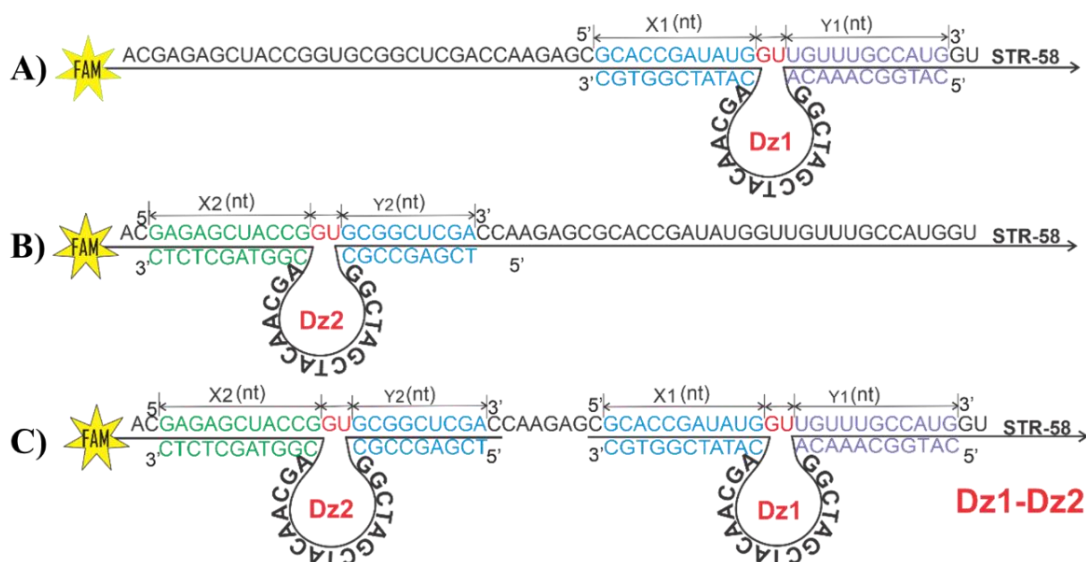


Figure 3. Design of Dz1 and Dz2. GU (red) site represent cleavage sites. X and Y are binding arms. X1 (blue) and X2 (green) are the binding arms at the 3' end of Dz1 and Dz2. Y1 (purple) and Y2 (blue) are the binding arms at the 5' end of Dz1 and Dz2. (A) Monovalent Dz1 cleaving at first cleavage site. (B) Monovalent Dz2 cleaving at second cleavage site. (C) Monovalent Dz1-Dz2 association cleaving at Dz1 and Dz2 cleavage sites.

3.3. Cleavage Efficiency of 10-23 DNAzymes (Dz1, Dz2 and Dz1-Dz2 Association)

To determine the most efficient system, we investigated the cleavage activity by incubating mRNA STR-58 with Dz1 and Dz2. The melting temperatures of the Dz1 binding arms X1 and Y1 were 32.4°C and 34.5°C respectively and that of Dz2 binding arms X2 and Y2 were 34.1°C and 34.9°C respectively. Our experiments were conducted in near physiological conditions (KCl = 150 mM, NaCl = 15 mM, MgCl₂ = 2 mM, HEPES = 50 mM, pH = 7.5 + 37°C) closer to humans. The substrate-binding arms aided in the association and dissociation of cleavage agents to the substrate by forming hydrogen bonds with a predetermined melting temperature. The melting temperature in this situation is the temperature at which 50% of one oligonucleotide is complementary bound to another. Samples were incubated for 1, 5, and 24 h.

Using STR-58 as target mRNA, we ran a multiple turnover experiment with cleavage agent concentrations of 10, 25, 50, and 100 nM. The concentration of targeted mRNA STR-58 was 1 μM. The samples were incubated at 37°C for 1, 5, and 24 h. After incubation, 20% PAGE electrophoresis (80V, 1, 5, and 24 h) was performed with three repetitions. The experiments were conducted in near physiological conditions (KCl = 150 mM, NaCl = 15 mM, MgCl₂ = 2 mM, HEPES = 50 mM, pH = 7.5 + 37°C) closer to humans. The results are depicted in figure 4 as graphs. The results were estimated using formula (1). By using formula (2), we converted the cleavage percentage results into catalytic turnover (h⁻¹).

$$\text{Turnover (-h)} = \frac{\text{percentage of cleavage RNA concentration}}{\text{cleavage agent concentration} \times \text{time} \times 100} \quad (2)$$

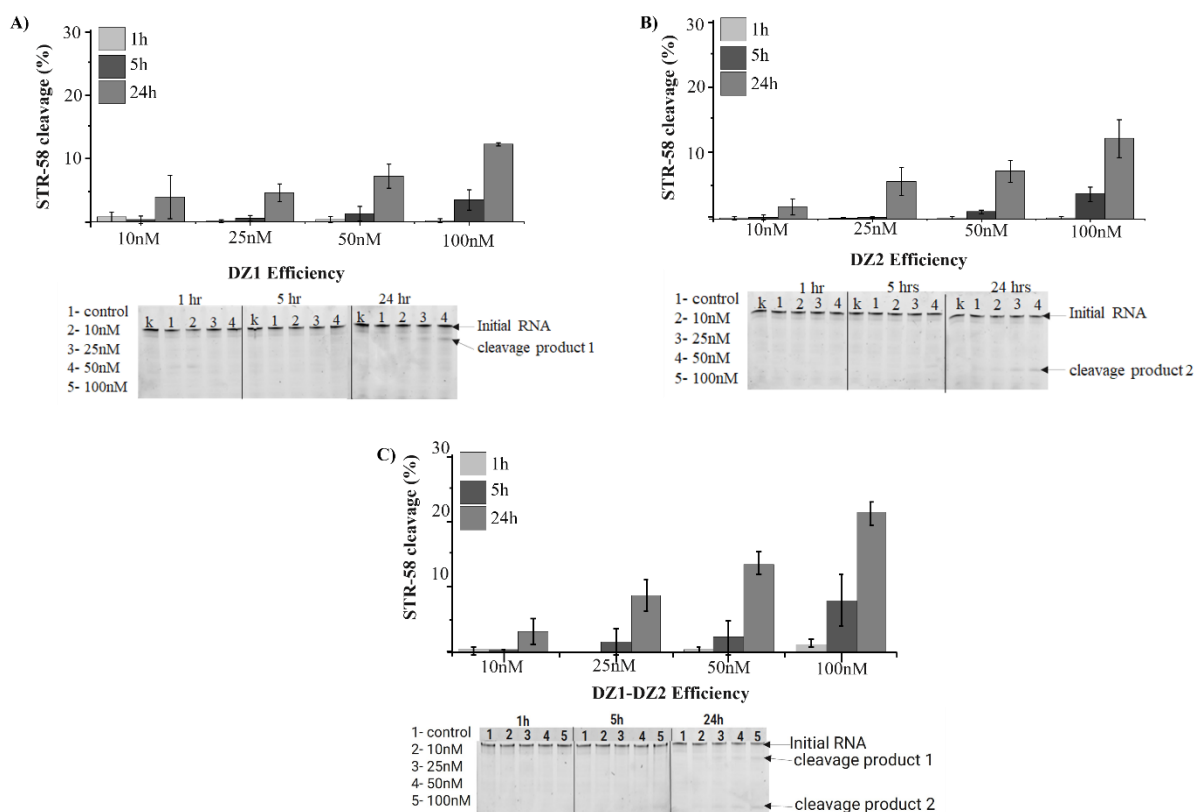


Figure 4. Relative cleavage of STR-58 RNA under multiple turnover condition. (A) DZ1 cleavage efficiency with STR-58 as a target. (B) DZ2 cleavage efficiency with STR-58 as a target. (C) Efficiency of DZ1-DZ2 association cleavage with STR-58 as a target. The result represents an average of at least 3 independent measurements.

The multiple turnover output showed that the incubation time affects the rate of catalysis. After 1 h of incubation, the lowest rate of cleavage was recorded, followed by 5 h and then 24 h. Cleavage efficiency is also influenced by the concentration of oligonucleotides. DZ1(3.9%) (0.16 h⁻¹), DZ2 (2.15%) (0.03 h⁻¹) and DZ1-DZ2 (3.3%) (0.14 h⁻¹) showed inefficient cleavage at 10 nM concentration after 24 h of incubation. As the concentration of oligonucleotides increased, the cleavage efficiency also increased. After 5 h of incubation, DZ1 had a 0.33% (0.07 h⁻¹), 0.53% (0.04 h⁻¹), 1.29% (0.05 h⁻¹), 3.45% (0.07 h⁻¹) cleavage efficiency at 10, 25, 50 and 100 nM respectively. DZ2 recorded 0.24% (0.05 h⁻¹), 0.23% (0.02 h⁻¹), 1.26% (0.05 h⁻¹), 4.4% (0.09 h⁻¹) cleavage efficiency at 10, 25, 50 and 100 nM respectively. At 10, 25, 50, and 100 nM, DZ1-DZ2 had cleavage efficiency of 0.3% (0.05 h⁻¹), 1.7% (0.1 h⁻¹), 2.3% (0.09 h⁻¹), 8.0% (0.16 h⁻¹), respectively.

At the end of 24 h of incubation, DZ1 at 100 nM concentrations was 12.3%, DZ2 was 14.27% and DZ1-DZ2 had 21.4% cleavage efficiency. When analyzing the efficiency of cleavage agents, we discovered that the concentration of oligonucleotides in a sample for catalytic cleavage activity is a key element to be considered. A sample with an insufficient amount of cleavage agent will have insufficient catalytic cleavage activity, resulting in ineffective knockdown of a targeted gene. Therefore, comparing the results, we found that multivalent association of DZ1-DZ2 performed better than monovalent DZ1 and DZ2. This finding shows that multivalent Dzs are more efficient than monovalents and hence paves a path for efficient knockdown of genes.

3.4. Optimization of DZ1, DZ2 and DZ1-DZ2 Association

To determine if two RNA-cleaving DNAzymes in a multivalent association provide advantages in RNA cleaving activity in comparison to two separate Dzs (DZ1 and DZ2),

modified Dz 10-23 with varied arm lengths (-/+1, +2 nucleotides less or more) were used to optimize the Dz1, Dz2 and Dz1-Dz2 association. (Figure 5). By adjusting the binding arms of Dz1 and Dz2, the melting temperatures change depending on nucleotide length. We conducted experiments with the Dz1, Dz2 and Dz1-Dz2 with different binding arms. Each binding arm length has a determined melting temperature that increases with the number of nucleotides in the binding arms. Table 3 has all the data for Dz1 and Dz2, including the lengths of their binding arms and related melting temperatures.

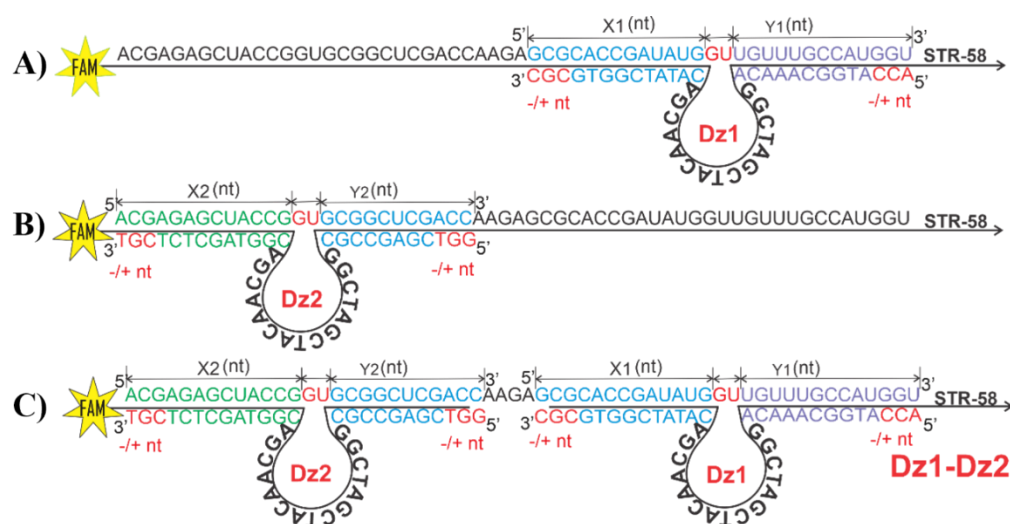


Figure 5. Chemically modified monovalent Dz 10-23. Dz 10-23 were by removal or addition of nucleotides (nt). Red sequence represents binding arm modifications and cleavage sites (GU). X1 (blue) and X2 (green) are the binding arms at the 3' end of Dz1 and Dz2. Y1 (purple) and Y2 (blue) are the binding arms at the 5' end of Dz1 and Dz2. (A) Monovalent Dz1 cleaving at first cleavage site. (B) Monovalent Dz2 cleaving at second cleavage site. (C) Monovalent Dz association cleaving at Dz1 and Dz2 cleavage sites. "nt" = nucleotide.

Table 3. The length nucleotides and melting temperature of Dz1 and Dz2 binding arms.

Name of Oligonucleotides	Length of 'X' Arm (nt)	Y arm T _m (°C)	Length of 'Y' Arm (nt)	X arm T _m (°C)
1	2	3	4	5
Dz1_10/10	10	26.2	10	23.4°C
Dz1-10/11	10	26.2	11	32.4°C
Dz1_11/10	11	32.3	10	23.4°C
Dz1_11/11	11	32.3	11	32.4
Dz1_11/12	11	32.3	12	39.6
Dz1_12/11	12	38.3	11	32.4
1	2	3	4	5
Dz1_12/12	12	38.3	12	39.6
Dz1_12/13	12	38.3	13	45.8
Dz1_13/12	13	40.7	12	39.6
Dz1_13/13	13	40.7	13	45.8
Dz2_8/10	8	28.3	10	28.7
Dz2_8/11	8	28.3	11	34.1
Dz2_9/10	9	34.9	10	28.7
Dz2_9/11	9	34.9	11	34.1
Dz2_9/12	9	34.9	12	41.2
Dz2_10/11	10	39.4	11	39.4

Dz2_10/12	10	39.4	12	41.2
Dz2_10/13	10	39.4	13	49.6
Dz2_11/12	11	45.3	12	41.2
Dz2_11/13	11	45.3	13	49.6

The cleavage agents were incubated for 5 h with STR-58 at 37°C. The relationship of concentration was 1 μM of STR-58 substrate to 100 nM (0.1 μM) Dz1, Dz2 and Dz1-Dz2. After incubation, we carried out 20% PAGE electrophoresis (80 V, 2 h). Densitometry was used to estimate the results, which were calculated using formula (1). The results are shown on the graphs in Figure 6. The result of Dz1 (Figure 6A) indicated an increase in cleavage efficiency as the binding arms increased. With 0.3% (0.01 h⁻¹) cleavage rates, Dz1_{10/10} and Dz1_{11/10} had the lowest cleavage rates. The design with the highest efficiency was Dz1_{12/13} (16.5% (0.4 h⁻¹)) followed by Dz1_{13/13} (16.2% (0.35 h⁻¹)). Considering the result for Dz2 (Figure 6B), the least cleavage was recorded in Dz2_{9/10} with a cleavage percentage of 0.2% (0.01 h⁻¹). The highest cleavage was demonstrated in Dz2_{11/12} (8.8% (0.1 h⁻¹)) followed by Dz2_{11/13} (8.6% (0.11 h⁻¹)). By 14.5%, Dz1_{12/13} outperformed Dz1_{11/11} (2.0%) (modified constructs). Dz2_{11/12} was 6.9% more efficient than Dz2_{9/11} (1.9%). These results demonstrate that the length of the binding arms influences the cleavage efficiency. Hence, increasing the length of the binding arms increases the cleavage efficiency of the substrate to the cleavage agent. The results from the Dz1-Dz2 (Figure 7A) association indicated multi ligand efficiency. We observed that Dz1_{10/10}-Dz2_{8/10} recorded the least cleavage (1.2% of cleavage). This is the design with the shortest binding arms. The cleavage efficiency increases as the nucleotides of the binding arms increase (Figures 6 and 7). This result also affirms the finding that the length of binding arms influences cleavage efficiency. Dz1_{12_13}-Dz2_{11/12} and Dz1_{13_13}-Dz_{11/12} had the highest cleavage efficiency of 21.0% and 20.9%, respectively, indicating statistically close catalytic activity.

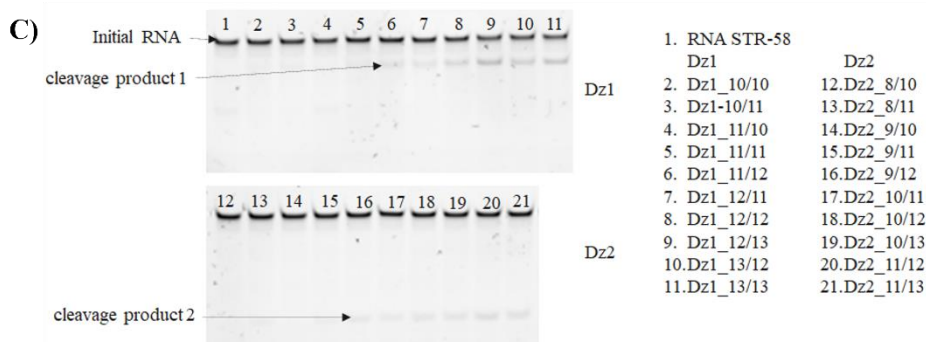
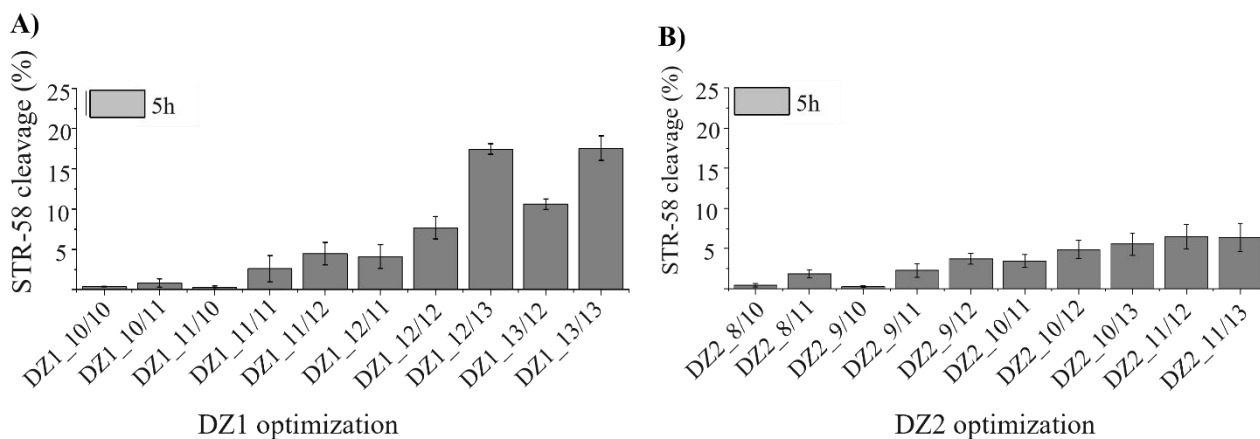


Figure 6. Optimization of Dz1 and Dz2 with varied binding arms and melting temperatures. (A) Dz1 optimization with varying binding arm lengths ranging from 10 to 13 nucleotides aimed at STR-58. (B) Dz2 optimization with a varied binding arm length of 8 to 13 nucleotides. (C) Optimization of Dz1 and Dz2 by PAGE electrophoresis.

The result is an indication of the Dz1_{12/13} and Dz2_{11/12} efficiency observed in the Dz1 and Dz2 optimization experiments (Figure 6). When comparing the result of Dz1_{12/13}-Dz2_{11/12} (modified cooperatively working) with Dz1_{11/11}-Dz2_{9/11} (initial cooperatively working construct), Dz1_{12/13}-Dz2_{11/12} was 17.2% more efficient than Dz1_{11/11}-Dz2_{9/11}(3.8%).

Therefore, in optimizing Dz1, Dz2 and Dz1-Dz2 association, our findings indicate that Dz1_{12/13}-Dz2_{11/12} has the highest catalytic cleavage activity, and we are sure that Dz1_{12/13}-Dz2_{11/12} with 12, 13, 11 and 12 binding arms is the optimized variant for monovalent STR-58-cleaving Dzs. To sum up about Dz 10-23 associations, we found that the addition of nucleotides to the binding arms enhances average catalytic cleavage. The experiments revealed preliminary rules for Dz 10-23 design to achieve the best possible catalytic efficiency. To establish preliminary rules that Dzs association increased catalytic cleavage, we needed to conduct Dzs kinetic studies. Therefore, we conducted experiments with Dz1_{12/13}, Dz2_{11/12}, and Dz1_{12/13}-Dz2_{11/12} to understand the chemical mechanism of Dzs' reaction to the targeted RNA (STR-58).

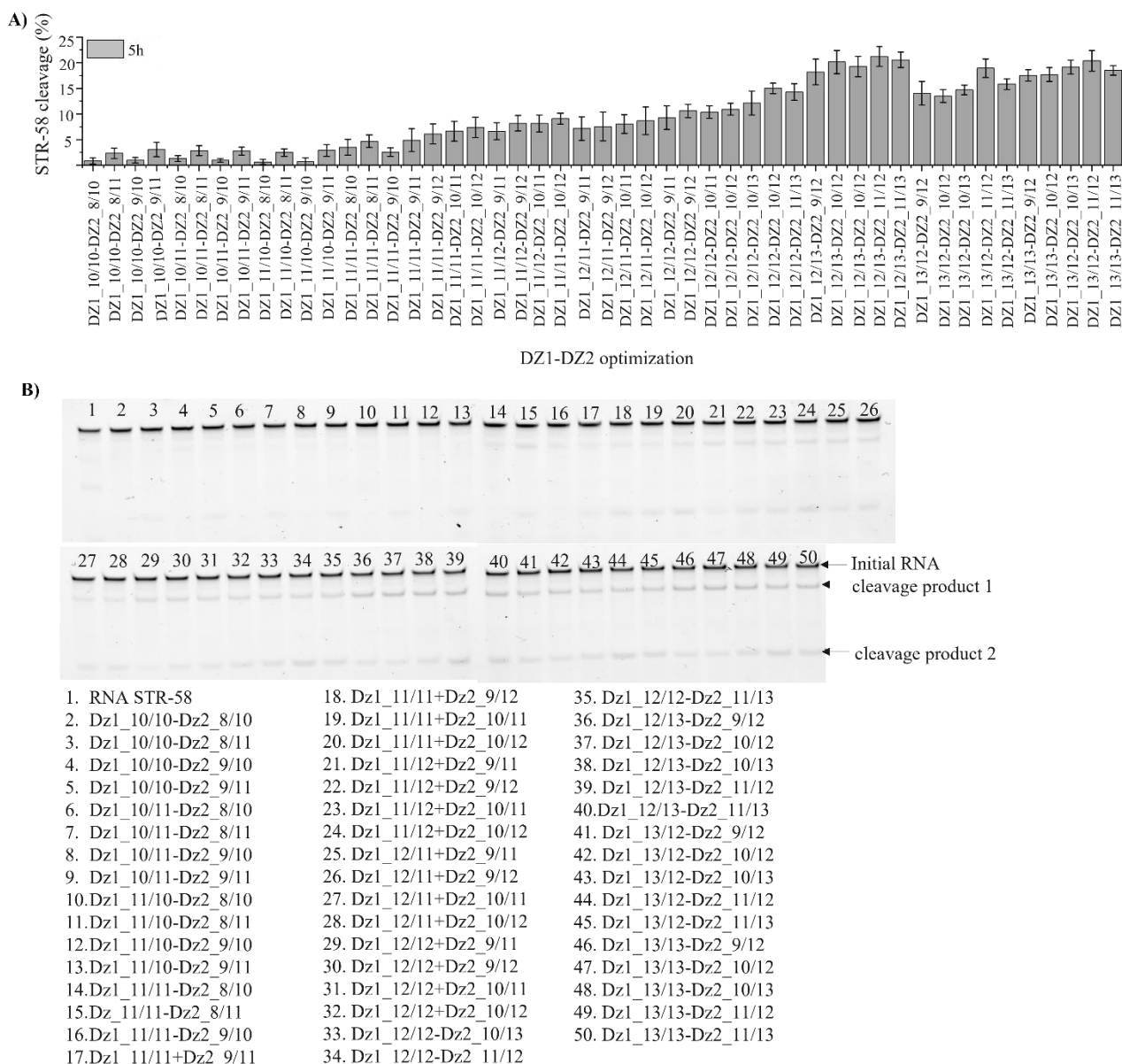


Figure 7. Optimization of Dz1-Dz2. (A) Result of Dz1-Dz2 optimization with varied binding arm length and melting temperature after 5 h of incubation. (B) PAGE electrophoresis of optimized Dz1-Dz2.

3.5. Discussion of Result

This study describes the practical application of a multivalent technique to enhance RNA-cleaving Dz 10-23 affinity and, hence, cleavage activity. The catalytic activity of DZs involves the interaction of a cleavage agent with a targeted substrate. It is well established that interaction of ligands with their binding sites results in binding affinity[19]. Biomolecules such as antibodies and other anti-inflammatory molecules use multiple binding sites to interact with ligands, which enhance their affinity for avidity. Avidity is the total binding strength of every binding site, which is determined by the binding affinity (the relationship at a singular binding site) and number of binding sites involved [20]. We used different cleavage agents' concentrations to understand the degree of effectiveness of 10-23 Dz. We observed an improved reaction rate in both Dz1, Dz2 and Dz1-Dz2 as the concentration of the cleavage agent increases demonstrating that concentration of enzymes influences biological processes. And hence, for effectively knocking down a targeted RNA

the concentration of the cleavage must be considered. Next, by optimizing Dz 10-23, we obtained the most effective Dz construct for kinetic analysis. It's known that optimization by chemical modification of Dz 10-23 in the binding arms' length influences Dz efficiency [21], [22]. We modified the ends of both the 3' and 5' arms by reducing the sequence by 1 nt or increasing it by 2 nt. Alternatively, the cleavage activity improved as we increased the length of the binding arm. This affirms that the length of the binding arms influences cleavage activity.

We achieved an optimized construct when the end of the 3' binding arm of Dz1 was increased to 12 nt and 5' to 13 nt. For Dz2, optimization was achieved when the 3' binding arm reached a length of 11 nt and the 5' binding to 12 nt. By cooperatively testing all the modified constructs in Dz1-Dz2 association, the catalytic efficiency was enhanced, and we achieved optimized Dz1_12/13-Dz2_11/12. We have established multivalent association of 10-23 Dz enhanced catalytic activity and efficiency.

4. Conclusion

We designed multivalent DNAzyme with the concept of multivalent ligands in nature and drug development to monovalent Dz to ascertain multivalent efficiency over monovalent Dzs. We obtained results indicating multivalent 10-23 Dz association efficiency. The result indicated that cooperative association of DNA increases hybridization and catalytic cleavage activity to STR-58. Our findings have demonstrated that multivalent Dzs hold the potential to increase DNAzyme-cleaving RNA affinity and efficiency as a therapeutic agent.

In summary, this study has demonstrated that

(1) Multivalent association of DNAzymes are higher in catalytic cleavage activity in cleaving STR-58 than monovalent constructions.

(2) Multivalent association of DNAzymes improves DNAzymes hybridization and affinity to targeted substrates, hence increasing their catalytic activity as compared to monovalent DNAzymes.

(3) Increasing the length of DZ 10-23 binding arms increased performance of DNAzymes.

Author Contributions:

Funding: The reported study was funded by Russian Foundation for Basic Research, project number 20-34-90071, Russian Science Foundation project number 22-24-00664 and the Priority 2030 Federal Academic Leadership Program.

Institutional Review Board Statement:

Informed Consent Statement:

Data Availability Statement:

Conflicts of Interest: The authors certify that there are no conflicts of interest regarding the submitted paper.

References

1. Kaufmann, S.H.E.; Dorhoi, A.; Hotchkiss, R.S.; Bartenschlager, R. Host-directed therapies for bacterial and viral infections. *Nat. Rev. Drug Discov.* **2018**, *17*, 35–56, doi: 10.1038/nrd.2017.162.
2. Lapteva, L.; Purohit-Sheth, T.; Serabian, M.; Puri, R.K. Clinical Development of Gene Therapies: The First Three Decades and Counting. *Mol. Ther. Methods Clin. Dev.* **2020**, *19*, 387–397, doi: 10.1016/j.omtm.2020.10.004.
3. Deverman, B.E.; Ravina, B.M.; Bankiewicz, K.S.; Paul, S.M.; Sah, D.W.Y. Gene therapy for neurological disorders: Progress and prospects. *Nat. Rev. Drug Discov.* **2018**, *17*, 641–659, doi: 10.1038/nrd.2018.110.
4. Moore, N.A.; Morral, N.; Ciulla, T.A.; Bracha, P. Gene therapy for inherited retinal and optic nerve degenerations. *Expert Opin. Biol. Ther.* **2018**, *18*, 37–49, doi: 10.1080/14712598.2018.1389886.

5. Pan, X.; *et al.* Applications and developments of gene therapy drug delivery systems for genetic diseases. *Asian J. Pharm. Sci.* **2021**, *16*, 687–703, doi: 10.1016/j.ajps.2021.05.003.
6. Vakulskas, C.A.; Behlke, M.A. Evaluation and Reduction of CRISPR Off-Target Cleavage Events. *Nucleic Acid Ther.* **2019**, *29*, 167–174, doi: 10.1089/nat.2019.0790.
7. Gonçalves, G.A.R.; Paiva, R.D.M.A. Gene therapy: Advances, challenges and perspectives," *Einstein (São Paulo)*, **2017**, *15*, 369–375, doi: 10.1590/s1679-45082017rb4024.
8. He, M.; *et al.* mRNA-activated multifunctional DNAzyme nanotweezer for intracellular mRNA sensing and gene therapy. *ACS Appl. Mater. Interfaces* **2021**, *13*, 8015–8025, doi: 10.1021/acsami.0c21601.
9. Xue, T.; Sheng, A.; Mao, D.; Zhang, Y.; Liu, Z.; Zhang, J. DNAzyme-based colorimetric assay and its application for lipopolysaccharide analysis assisted by oxime chemistry. *Biosens. Bioelectron.* **2021**, *189*, 113379, doi: 10.1016/j.bios.2021.113379.
10. Watts, J.K.; Corey, D.R. Silencing disease genes in the laboratory and the clinic. *J. Pathol.* **2012**, *226*, 365–379, doi: 10.1002/path.2993.
11. Warashina, M.; Kuwabara, T.; Kato, Y.; Sano, M.; Taira, K. RNA–protein hybrid ribozymes that efficiently cleave any mRNA independently of the structure of the target RNA. *Proc. Natl. Acad. Sci.* **2001**, *98*, 5572–5577, doi: 10.1073/pnas.091411398.
12. Böhmer, V.I.; Szymanski, W.; Feringa, B.L.; Elsinga, P.H. Multivalent Probes in Molecular Imaging: Reality or Future? *Trends Mol. Med.* **2021**, *27*, 379–393, doi: 10.1016/j.molmed.2020.12.006.
13. Kim, H.; Choi, H.; Heo, Y.; Kim, C.; Kim, M.; Kim, K.T. Biosensors Based on Bivalent and Multivalent Recognition by Nucleic Acid Scaffolds. *Appl. Sci.*, **2022**, *12*, 1717, doi: 10.3390/app12031717.
14. Bernardi, A. *et al.* Multivalent glycoconjugates as anti-pathogenic agents. *Chem. Soc. Rev.* **2013**, *42*, 4709–4727, doi: 10.1039/c2cs35408j.
15. Yang, D.K.; Kuo, C.J.; Chen, L.C. Synthetic multivalent DNAzymes for enhanced hydrogen peroxide catalysis and sensitive colorimetric glucose detection. *Anal. Chim. Acta* **2015**, *856*, 96–102, doi: 10.1016/j.aca.2014.11.031.
16. Chen, F.; *et al.* Inhibition of ampicillin-resistant bacteria by novel mono-DNAzymes and di-DNAzyme targeted to beta-lactamase mRNA. *Oligonucleotides* **2004**, *14*, 80–89, doi: 10.1089/1545457041526308.
17. Sunde, M.; Norström, M. The genetic background for streptomycin resistance in *Escherichia coli* influences the distribution of MICs. *J. Antimicrob. Chemother.* **2005**, *56*, 87–90, doi: 10.1093/jac/dki150.
18. Lee, Y.S.; Kim, G.H.; Koh, Y.J.; Jung, J.S. Identification of strA–strB Genes in Streptomycin-Resistant *Pseudomonas syringae* pv. *actinidiae* Biovar 2 Strains Isolated in Korea. *Plant. Pathol. J.* **2021**, *37*, 489–493, doi: 10.5423/ppj.nt.05.2021.0078.
19. Du, X.; *et al.*, Insights into Protein-Ligand Interactions: Mechanisms, Models, and Methods. *Int. J. Mol. Sci.*, **2016**, *17*, doi: 10.3390/ijms17020144.
20. Rudnick, S.I.; Adams, G.P. Affinity and avidity in antibody-based tumor targeting. *Cancer Biother. Radiopharm.*, **2009**, *24*, 155–161, doi: 10.1089/cbr.2009.0627.
21. Schubert, S.; Gül, D.C.; Grunert, H.-P.; Zeichhardt, H.; Erdmann, V.A.; Kurreck, J. RNA cleaving '10-23' DNAzymes with enhanced stability and activity. *Nucleic Acids Res.* **2003**, *31*, 982–992, doi: 10.1093/nar/gkg791.
22. Su, D.; Zhang, D. Linker Design Impacts Antibody-Drug Conjugate Pharmacokinetics and Efficacy via Modulating the Stability and Payload Release Efficiency. *Front. Pharmacol.* **2021**, *12*, doi: 10.3389/fphar.2021.687926.